Cell

Identification of Selective Inhibitors of Cancer Stem Cells by High-Throughput Screening

Piyush B. Gupta,[1,3,7,*] Tamer T. Onder,[1,2,7] Guozhi Jiang,[1,3] Kai Tao,[4] Charlotte Kuperwasser,[4] Robert A. Weinberg,[1,2,6,8,*] and Eric S. Lander[1,2,3,5,8,*]

[1]Department of Biology, Massachusetts Institute of Technology, Cambridge, MA 02139, USA
[2]Whitehead Institute for Biomedical Research, 9 Cambridge Center, Cambridge, MA 02142, USA
[3]Broad Institute of MIT and Harvard, Cambridge, MA 02142, USA
[4]Department of Anatomy and Cell Biology, Tufts University School of Medicine and Molecular Oncology Research Institute, Tufts Medical Center, Boston, MA 02111, USA
[5]Department of Systems Biology, Harvard Medical School, Boston, MA 02115, USA
[6]MIT Ludwig Center for Molecular Oncology, Cambridge, MA 02139
[7]These authors contributed equally to this work
[8]These authors contributed equally to this work
*Correspondence: piyush@broadinstitute.org (P.B.G.), weinberg@wi.mit.edu (R.A.W.), lander@broadinstitute.org (E.S.L.)
DOI 10.1016/j.cell.2009.06.034

SUMMARY

Screens for agents that specifically kill epithelial cancer stem cells (CSCs) have not been possible due to the rarity of these cells within tumor cell populations and their relative instability in culture. We describe here an approach to screening for agents with epithelial CSC-specific toxicity. We implemented this method in a chemical screen and discovered compounds showing selective toxicity for breast CSCs. One compound, salinomycin, reduces the proportion of CSCs by >100-fold relative to paclitaxel, a commonly used breast cancer chemotherapeutic drug. Treatment of mice with salinomycin inhibits mammary tumor growth in vivo and induces increased epithelial differentiation of tumor cells. In addition, global gene expression analyses show that salinomycin treatment results in the loss of expression of breast CSC genes previously identified by analyses of breast tissues isolated directly from patients. This study demonstrates the ability to identify agents with specific toxicity for epithelial CSCs.

INTRODUCTION

Studies have identified subpopulations of cells within tumors that drive tumor growth and recurrence, termed cancer stem cells (CSCs) (Al-Hajj et al., 2003; Lapidot et al., 1994; Li et al., 2008; Singh et al., 2003; Smalley and Ashworth, 2003; Stingl and Caldas, 2007). CSCs are resistant to many current cancer treatments, including chemo- and radiation therapy (Bao et al., 2006; Dean et al., 2005; Diehn et al., 2009; Diehn and Clarke, 2006; Eyler and Rich, 2008; Li et al., 2008; Woodward et al., 2007). This suggests that many cancer therapies, while killing the bulk of tumor cells, may ultimately fail because they do not eliminate CSCs, which survive to regenerate new tumors.

CSC representation in cancer cell populations is operationally measured based on the ability to seed tumors at limiting dilutions in vivo. CSC-enriched cancer cell populations also exhibit certain properties in vitro: (1) CSC-enriched subpopulations can be isolated with cell-surface marker profiles (Al-Hajj et al., 2003; Li et al., 2007a; Ricci-Vitiani et al., 2007; Singh et al., 2003; Zhang et al., 2008); for example, breast CSCs are enriched in the $CD44^{high}/CD24^{low}$ subfraction of cells (Al-Hajj et al., 2003). (2) CSC-enriched populations form spherical colonies in suspension cultures, termed tumor mammospheres (Dontu et al., 2003) or tumorspheres. (3) CSC-enriched populations exhibit increased resistance to chemotherapeutic agents (Bao et al., 2006; Dean et al., 2005; Diehn and Clarke, 2006; Eyler and Rich, 2008; Li et al., 2008; Woodward et al., 2007) and ionizing radiation (Diehn et al., 2009; Woodward et al., 2007).

In principle, the application of automated screening technologies could facilitate the identification of agents that kill CSCs. However, since CSCs generally comprise only small minorities within cancer cell populations, standard high-throughput cell viability assays applied to bulk populations of cancer cells cannot identify agents with CSC-specific toxicity. Accordingly, screening for agents that preferentially kill CSCs depends on the ability to propagate stable, highly enriched populations of CSCs in vitro. However, this is not currently possible for the CSCs of solid tumors. For example, breast CSC enrichment is rapidly lost during in vitro culture (Fillmore and Kuperwasser, 2008).

The induction of an epithelial-mesenchymal transition (EMT) in normal or neoplastic mammary epithelial cell populations has been shown to result in the enrichment of cells with stem-like properties (Mani et al., 2008). We demonstrate here that normal and cancer cell populations experimentally induced into an EMT also exhibit an increased resistance to chemotherapy drug treatment. We exploit this observation to develop and implement

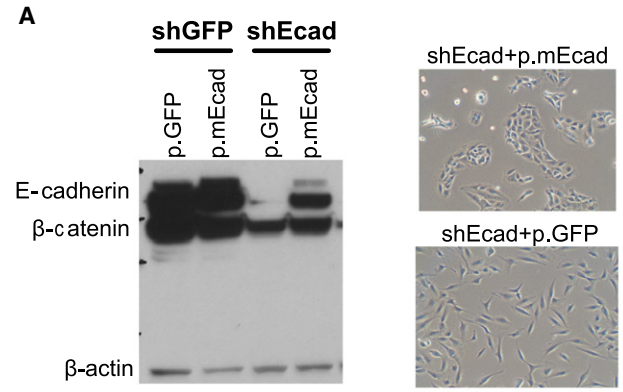

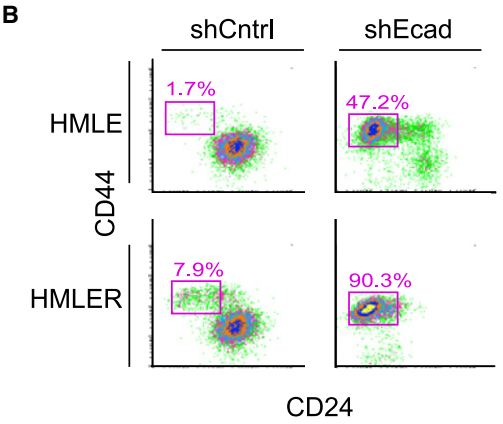

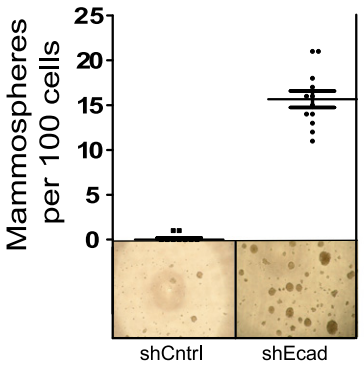

D

Tumor Seeding

Cells injected	HMLER shCntrl	HMLER shEcad
$1x10^6$	8/10	10/10
$1x10^5$	3/4	4/4
$1x10^4$	1/4	4/4
$1x10^3$	0/4	4/4

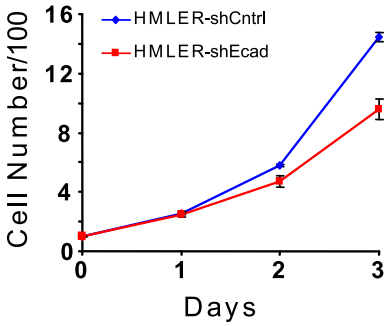

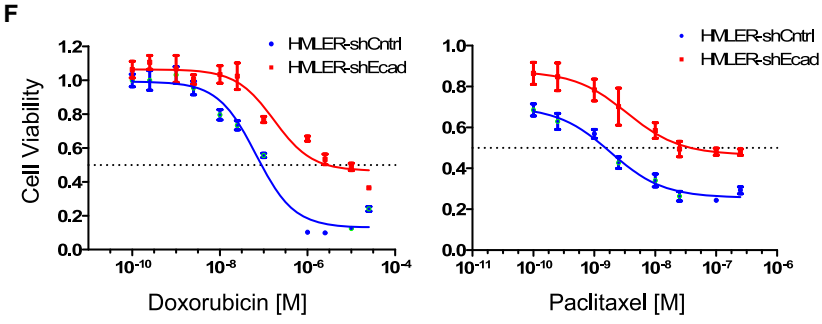

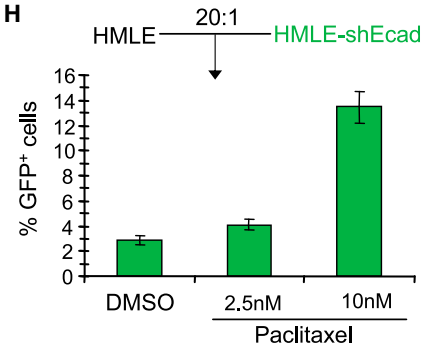

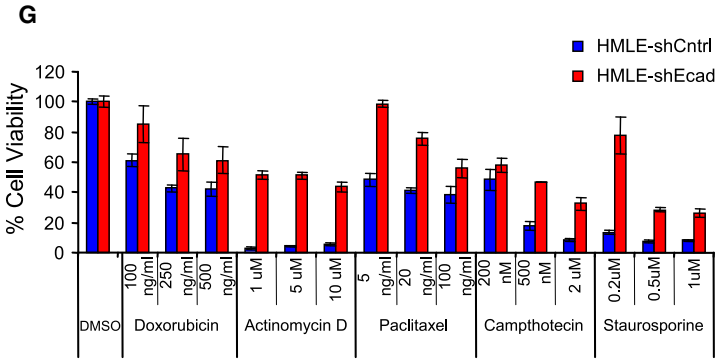

a high-throughput screening method to identify agents with specific toxicity for epithelial CSCs. The results of our screen and subsequent experiments demonstrate that it is possible to find agents with strong selective toxicity for breast CSCs.

RESULTS

CSC Numbers Are Increased in Breast Cancer Cells Induced into an EMT

We sought to increase the proportion of CSCs in breast cancer cell populations by inducing them to pass through an EMT. To this end, we modified experimentally transformed HMLER breast cancer cells (Elenbaas et al., 2001) by short hairpin RNA (shRNA)-mediated inhibition of the human *CDH1* gene, which encodes E-cadherin. Confirming previous results, an shEcad vector triggered an EMT and resulted in acquisition of a mesenchymal phenotype (Figure 1A) (Onder et al., 2008). Moreover, expression of a murine E-cadherin gene resistant to the introduced human shEcad construct caused reversion of EMT-associated phenotypes, indicating that EMT induction was not due to off-target shRNA effects (Figure 1A).

We next examined whether HMLER cancer cell populations induced through an EMT displayed an increase in the proportion of cells carrying the $CD44^{high}/CD24^{low}$ marker profile associated with human mammary CSCs. We observed that the percentage of $CD44^{high}/CD24^{low}$ cells was ~10-fold higher in $HMLER^{shEcad}$ cells than in control cells ($HMLER^{shCntrl}$) (~90% versus 8%; Figure 1B). A similar increase was observed in HMLER cells induced to undergo EMT by expression of Twist, a transcription factor whose ability to program an EMT is well documented (Mani et al., 2008; Yang et al., 2004).

We next tested the ability of $HMLER^{shEcad}$ cells to form tumorspheres when grown in suspension cultures, an in vitro measure of CSC activity. $HMLER^{shEcad}$ cells showed an ~100-fold increase in tumorsphere-forming ability relative to $HMLER^{shCntrl}$ cells (15 spheres versus ~0.15 spheres per 100 cells; Figure 1C). We also directly assayed the ability of $HMLER^{shEcad}$ cells to seed tumors in mice. Tumors were generated with 1000 $HMLER^{shEcad}$ cells, which was 100-fold less than was required for tumor seeding by $HMLER^{shCntrl}$ cells (Figure 1D). While displaying increased CSC activity, the $HMLER^{shEcad}$ cells proliferated more slowly than the $HMLER^{shCntrl}$ cells (Figure 1E). Thus, using all established measures of CSC activity, HMLER breast cancer cell populations that had undergone an EMT contained a significantly greater proportion of CSCs relative to control cell populations.

Normal and Neoplastic Cells Induced to Pass through an EMT Exhibit Increased Drug Resistance

Drug treatment of cancer cell populations leads to a concomitant enrichment for CSCs (Levina et al., 2008) and for cells that have undergone an EMT (Eyler and Rich, 2008; Thomson et al., 2005; Yang et al., 2006; Yauch et al., 2005). We therefore examined whether breast cancer cell populations that have been experimentally induced into EMT also share this aspect of CSC biology, namely an increased resistance to chemotherapeutic drugs. We found that $HMLER^{shEcad}$ cells were more resistant than $HMLER^{shCntrl}$ cells to two commonly used chemotherapeutic drugs, paclitaxel (~20-fold increase in IC_{50}) and doxorubicin (~5-fold increase) (Figure 1F). Taken together with the above observations, these findings indicated that breast cancer cell populations induced into EMT were operationally indistinguishable from populations enriched for CSCs using cell-surface markers.

Cancer cells often carry uncharacterized genetic alterations, some of which could contribute in important ways to the increased drug resistance observed after EMT induction. We therefore examined whether untransformed epithelial cells also exhibited increased drug resistance after EMT induction. We studied HMLE cells, which are immortalized mammary epithelial cells that differ from HMLER cells in that they lack an introduced *HrasV12* oncogene and are nontumorigenic. Similar to the transformed $HMLER^{shEcad}$ cells, when E-cadherin was downregulated in these cells through shRNA-mediated inhibition, the resulting $HMLE^{shEcad}$ cells underwent an EMT and were found to contain an ~80-fold increase in the proportion of $CD44^{high}/CD24^{low}$ cells relative to $HMLE^{shCntrl}$ controls (Figure 1B). In addition, like $HMLER^{shEcad}$ cells, the nontumorigenic $HMLE^{shEcad}$ cells exhibited increased resistance (10- to 20-fold) to paclitaxel and doxorubicin relative to control cells not induced into EMT (Figure 1G). In fact, $HMLE^{shEcad}$ cells were also more resistant than $HMLE^{shCntrl}$ cells to other established chemotherapeutic drugs, including actinomycin D, camptothecin, and staurosporine, a broad-spectrum kinase inhibitor (Figure 1G). These results indicated that the increased drug resistance observed after EMT induction is not a consequence of neoplastic transformation.

We next examined whether the increased drug resistance associated with cells induced to pass through an EMT would

Figure 1. Mesenchymally Transdifferentiated Breast Epithelial Cells Have Increased Numbers of CSCs and Are Drug Resistant

(A) Western blotting for E-cadherin, β-catenin, and β-actin in HMLER cells expressing shRNA against either GFP (shGFP) or the human *CDH1* gene (shEcad). Stable introduction of a murine *ECAD* gene (p.mEcad) but not GFP (p.GFP) results in re-expression of E-cadherin protein and reversal of EMT-associated morphology.

(B) FACS with CD24 and CD44 markers. The percentage of the $CD44^{+}/CD24^{-}$ subpopulation is indicated.

(C and D) Mammosphere formation assays (C) and tumor-seeding (D) with HMLERshCntrl and HMLERshEcad breast cancer cells. Bars in (C) denote the standard error (n = 12).

(E) Proliferation curves of HMLER-shCntrl and HMLER-shEcad cells grown in culture. Viable cells were counted by Trypan Blue dye exclusion. Bars denote the standard error (n = 5).

(F) Dose-response curves of HMLERshEcad and HMLERshCntrl breast cancer cells treated with doxorubicin or paclitaxel. Bars denote the standard error (n = 5).

(G) Viability of immortalized, non-tumorigenic breast epithelial cells (HMLE shCntrl) and cells induced through EMT (HMLEshEcad) treated with various chemotherapy compounds. Bars denote the standard error (n = 5).

(H) Proportion by FACS of GFP-labeled HMLEshEcad cells after paclitaxel treatment when mixed with control cells (HMLE) cells. Bars denote the standard error (n = 3).

select for the preferential outgrowth of such cells after drug treatment in vitro. Accordingly, we treated cocultures of green fluorescent protein (GFP)-labeled HMLE^{shEcad} cells and unlabeled, unfractionated HMLE^{shCntrl} cells (1:20 ratio) with paclitaxel in culture. Treatment for 4 days with paclitaxel (10 nM) resulted in a 4-fold increase in the proportion of HMLE^{shEcad} cells compared to DMSO-treated cocultures (Figure 1H), indicating that paclitaxel treatment leads to the selective outgrowth of cells that have undergone an EMT.

Identification via High-Throughput Screening of Compounds with EMT-Specific Toxicity

The results above indicated that (1) breast cancer cells that have undergone an EMT exhibited an ~100-fold increase in CSCs and that (2) the responses of immortalized nontumorigenic epithelial cells (HMLE) to drug treatment closely paralleled the drug treatment responses of their neoplastically transformed HMLER derivatives. Having also observed that HMLE^{shEcad} cells exhibit increased resistance to commonly used chemotherapeutic drugs, we speculated that agents that selectively target these nontransformed cells might also be found subsequently to exhibit selective toxicity toward CSCs.

Based on this reasoning, we designed a proof-of-concept screen to identify agents that selectively target mesenchymally transdifferentiated breast epithelial cells. We therefore screened test compounds for their effects on HMLE^{shEcad} and control HMLE^{shCntrl} cells. Cells from each cell line were seeded in 384-well plates, allowed to proliferate for 1 day, treated with test compounds, and assayed for cell viability 3 days later with a luminescence assay; compounds were screened in duplicate for each cell line (Figure 2A; Experimental Procedures). We screened a collection of ~16,000 compounds, which included several diverse commercial libraries, as well as collections of natural extracts; many of the compounds in these collections had known bioactivity (Experimental Procedures).

About 10% of the tested compounds reduced the viability of HMLE^{shEcad} cells, but the vast majority (98%) of this set of compounds also reduced the viability of the control HMLE^{shCntrl} cells. Only 32 compounds (~0.2% of total library) exhibited selective toxicity toward the HMLE^{shEcad} cells (Figure 2B). Among the ~100 commonly used chemotherapeutic drugs contained in this large compound library, the proportion of hits was not significantly higher, with only three showing any evidence of selective toxicity toward the HMLE^{shEcad} cells.

We selected eight of these 32 compounds for further study, based on their availability, and evaluated their effects across a range of doses. Upon retesting, four of these eight compounds showed consistent evidence of selective toxicity toward HMLE^{shEcad} cells (Figure 3A). The chemical identities of these four compounds were confirmed with high-resolution mass spectrometry (data not shown). Three of these compounds (etoposide, salinomycin, and abamectin) showed moderate-to-strong selectivity (IC_{50} ~10-fold lower for HMLE^{shEcad} cells than HMLE^{shCntrl} cells); the fourth, nigericin, showed more modest selectivity (~7-fold). The four compounds that selectively inhibited the immortalized HMLE^{shEcad} human mammary epithelial cells also preferentially killed cells that had undergone an EMT because of forced expression of the Twist transcription factor (HMLE^{Twist}; Figure 3B; Figure S1 available online). Thus, the dose-response curves of these four compounds for HMLE^{Twist} cells were essentially identical to those observed for HMLE^{shEcad} cells (Figure 3B). These results suggest that the selectivity of these compounds is independent of the particular mechanism used to induce mesenchymal transdifferentiation and the associated acquisition of stem cell traits.

While these four compounds were identified as selective inhibitors of immortalized human breast epithelial cells (HMLE^{shEcad}) that had undergone an EMT, it was not clear whether they would also exhibit a selective effect on the corresponding tumorigenic cells (HMLER^{shEcad}). In fact, across a range of concentrations, salinomycin was selectively toxic for the HMLER^{shEcad} cells (~8-fold selectivity), while the remaining three compounds (abamectin, etoposide, and nigericin) displayed only a modest selective toxicity (~2-fold) toward the HMLER^{shEcad} cells, in all cases relative to the HMLER^{shCntrl} cells (Figure 3C).

Salinomycin Selectively Kills Breast CSCs

In response to these various observations, we focused our further investigations on the properties of salinomycin. We observed that the sensitivity of breast cancer cell lines to salinomycin correlated with the relative abundance of their CD44^{high}/CD24^{low} CSC-enriched subpopulations (Figure S2). Accordingly, we sought to assess the specific effects of salinomycin on CSCs that existed naturally as a subpopulation within HMLER breast cancer cells rather than in populations experimentally induced into an EMT. For these and subsequent compound-treatment experiments, we treated cells for a specified time, allowed cells to recover for 4 days, and then conducted subsequent experimental assays in the absence of additional treatment, since this protocol would ensure that any further toxicity in the continued presence of a chemical compound would not confound the results of assays used to measure CSC representation.

We first assayed the effects of treatment on the proportion of breast cancer cells with the CD44^{high}/CD24^{low} antigenic phenotype (Al-Hajj et al., 2003). Salinomycin treatment decreased the proportion of CD44^{high}/CD24^{low} breast cancer cells by 20-fold relative to vehicle-treated controls; in contrast, paclitaxel treatment increased the proportion by 18-fold. The relative size of the CD44^{high}/CD24^{low} fraction was therefore 360-fold lower after treatment with salinomycin than with paclitaxel (HMLER_1, Figure 4A). In a second experiment with an independent population of HMLER breast cancer cells that naturally contains a high proportion of CSCs, we observed an ~75-fold reduction in the proportion of CSCs after salinomycin treatment compared to control treatment (HMLER_2, Figure 4A). We observed comparable results with cells of the SUM159 human breast carcinoma line (Figure S3).

As a functional measure of CSC frequency, we also examined the ability of HMLER breast cancer cells to form tumorspheres after treatment with salinomycin, paclitaxel, or dimethyl sulfoxide (DMSO) control. Salinomycin treatment induced an ~10-fold decrease in the number of tumorspheres relative to controls (Figure 4B). In contrast, paclitaxel treatment did not affect the number of tumorspheres formed, resulting instead in a significant increase in tumorsphere size.

We speculated that the inability of paclitaxel treatment to increase relative tumorsphere numbers was due to the already

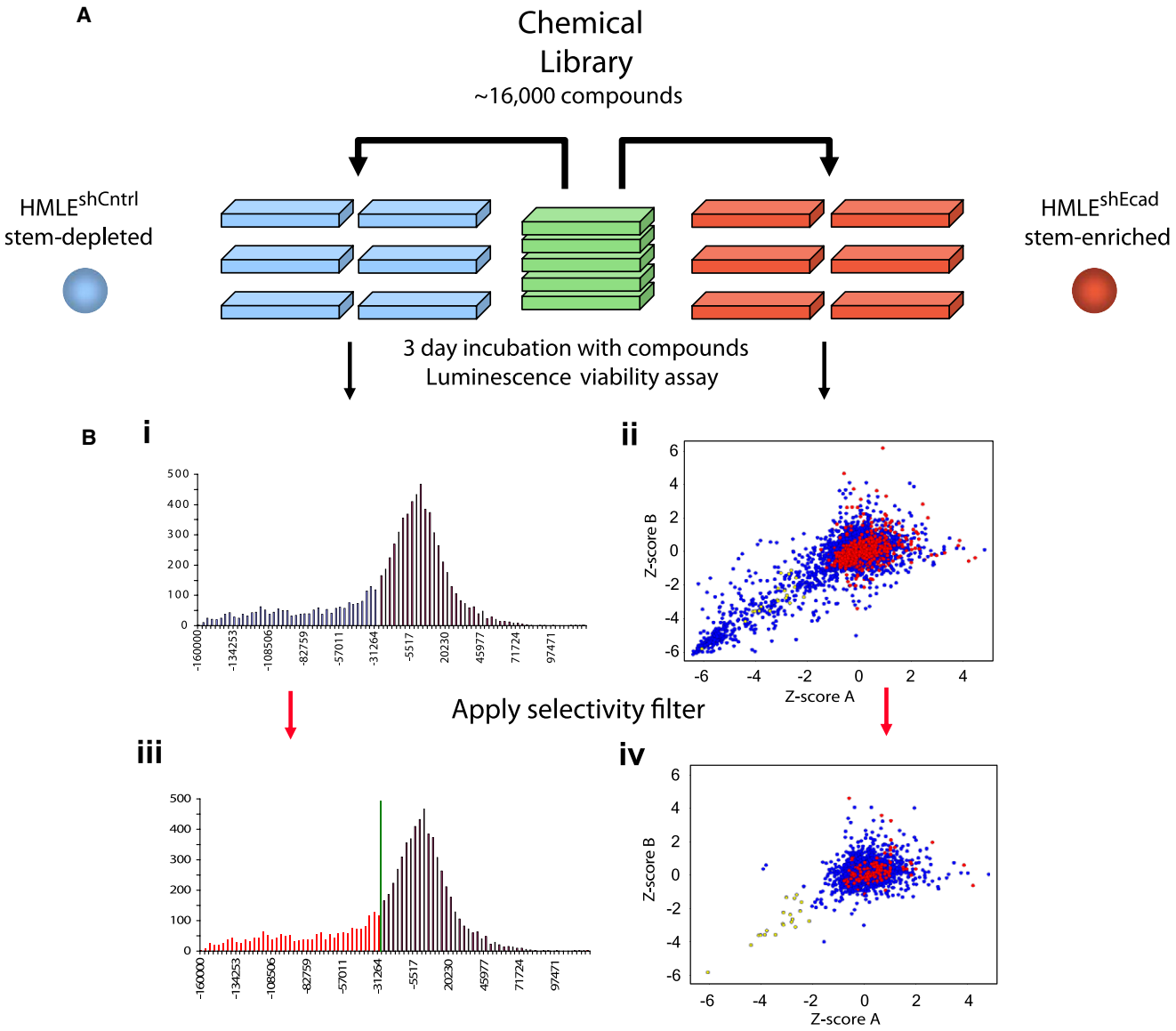

Figure 2. Chemical Screening for Compounds that Selectively Kill Mesenchymally Transdifferentiated Immortalized Epithelial Cells

(A) Schematic of the screen design and protocol.

(B) (i) Histogram of replicate-averaged background-corrected viability signal intensities (see the Experimental Procedures for details) for the viability of each tested compound for control breast epithelial cells (HMLE^{shCntrl}). Low/high signal intensities indicate compounds that reduce/increase cell viability. (ii) XY-Scatter plot of normalized Z scores for the viability of each tested compound for mesenchymally transdifferentiated breast epithelial cells (HMLE^{shEcad}; red dots indicate DMSO treatment; blue dots indicate test compounds). "Z-scoreA" and "Z-scoreB" represent the normalized Z scores for the two independent replicates of the screen. (iii) The data are as in (i) with the red shaded region in the histogram representing compounds that exhibited mild-to-strong toxicity (>1 SD lower than the mean normalized signal intensity) for the control HMLE^{shCntrl} epithelial cells. Compounds within the red region in (iii) were filtered out of the plot in (ii), producing the scatter plot in (iv). Application of this selectivity filter resulted in the identification of compounds that selectively killed mesenchymally transdifferentiated HMLE^{shEcad} but not control HMLE^{shCntrl} epithelial cells (yellow dots).

high proportion of CSCs present in the HMLER breast cancer cell line used in this assay. To address this issue directly, we controlled the proportion of CSCs in the test population by reconstructing a mixed population of CSCs and non-CSCs; we did this by admixing cells that had been forced to undergo an EMT with control cells that had not undergone this transition. This resulted in a representation of CSCs that allowed both positive and negative effects on CSC numbers to be assayed within a single cancer cell population (termed HMLER_Mx).

Salinomycin treatment decreased the proportion of CD44^{high}/CD24^{low} HMLER_Mx cells by 4-fold relative to vehicle-treated controls; in contrast, paclitaxel treatment increased the proportion of CD44^{high}/CD24^{low} HMLER_Mx cells by 4-fold. The relative proportion of CD44^{high}/CD24^{low} HMLER_Mx cells was therefore

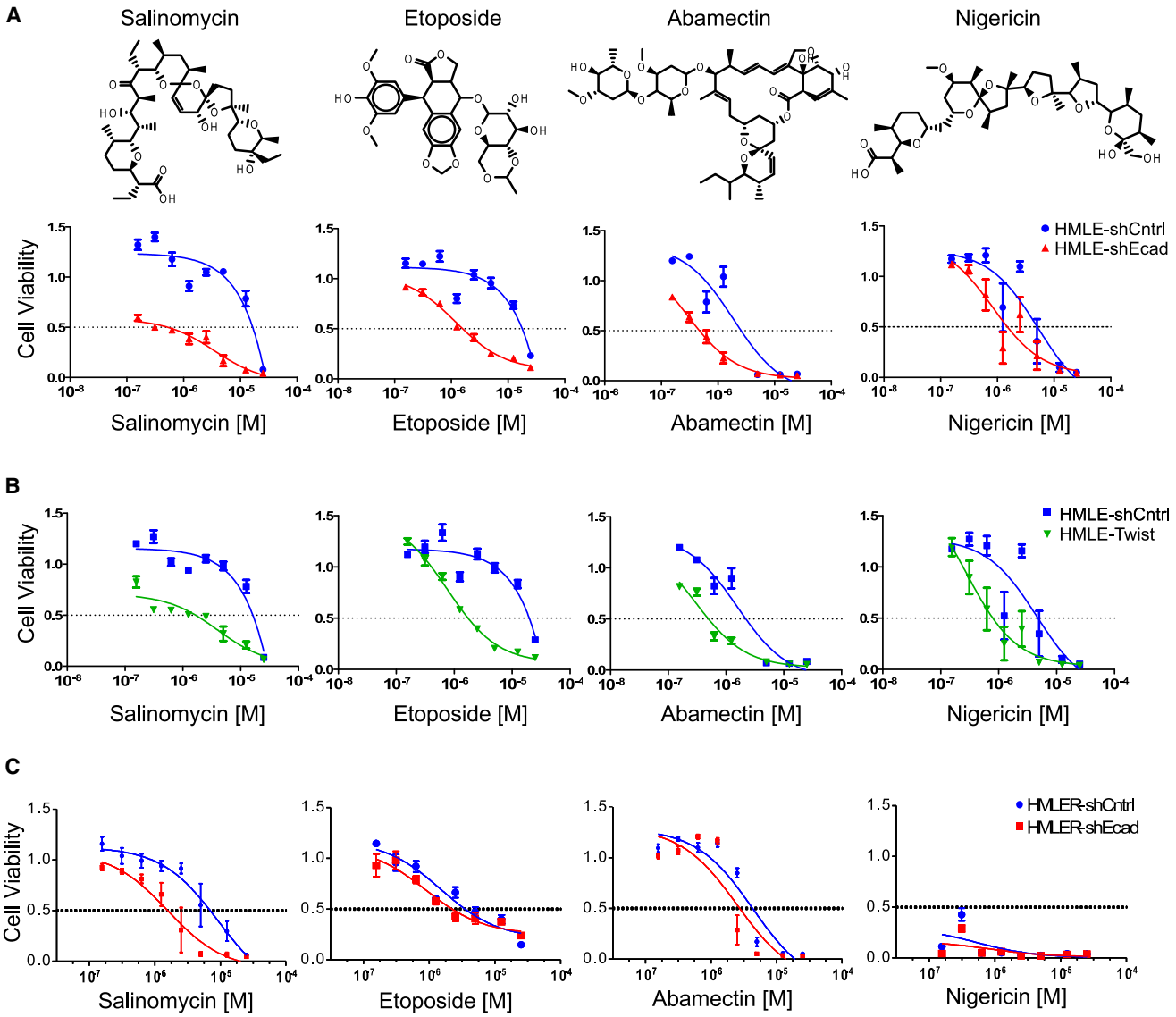

Figure 3. Identification and Validation of Compounds that Exhibit Selective Toxicity for Mesenchymally Transdifferentiated Epithelial Cells

(A) Chemical structure of salinomycin, etoposide, abamectin, and nigericin and dose-response curves of control HMLE-shCntrl cells and HMLE-shEcad cells treated with indicated compounds.

(B) Dose-response curves of the viability of HMLE-shCntrl and HMLE-Twist cells.

(C) Dose-response curves of control HMLER and HMLER-shEcad tumorigenic mammary epithelial cells treated with salinomycin, etoposide, abamectin, or nigericin.

Bars denote the standard error with n = 6 for each treatment combination.

16-fold lower after treatment with salinomycin than with paclitaxel (Figure 4C). Similarly, treatment of immortalized nontumorigenic HMLE_Mx cells with salinomycin reduced the fraction of $CD44^{high}/CD24^{low}$ HMLE_Mx cells 4-fold, whereas paclitaxel treatment increased the fraction of $CD44^{high}/CD24^{low}$ HMLE_Mx cells 4-fold (Figure 4C).

We also examined the effects of drug treatment on the ability of either breast cancer (HMLER_Mx) or immortalized mammary epithelial (HMLE_Mx) cells to form colonies in suspension culture. Sphere-forming ability in suspension cultures is correlated with CSC numbers in cancer cell lines and with progenitor activity in untransformed mammary epithelial cells (Dontu et al., 2003). Salinomycin treatment resulted in a 13-fold decrease in the number of HMLER_Mx tumorspheres relative to controls (Figure 4D). In contrast, paclitaxel treatment induced a 2-fold increase in the number of HMLER_Mx tumorspheres relative to vehicle treatment; as before, paclitaxel also caused a significant increase in HMLER_Mx tumorphere size (Figure 4D).

Salinomycin treatment also reduced mammosphere formation by nontumorigenic HMLE_Mx populations (>10-fold; Figure 4D).

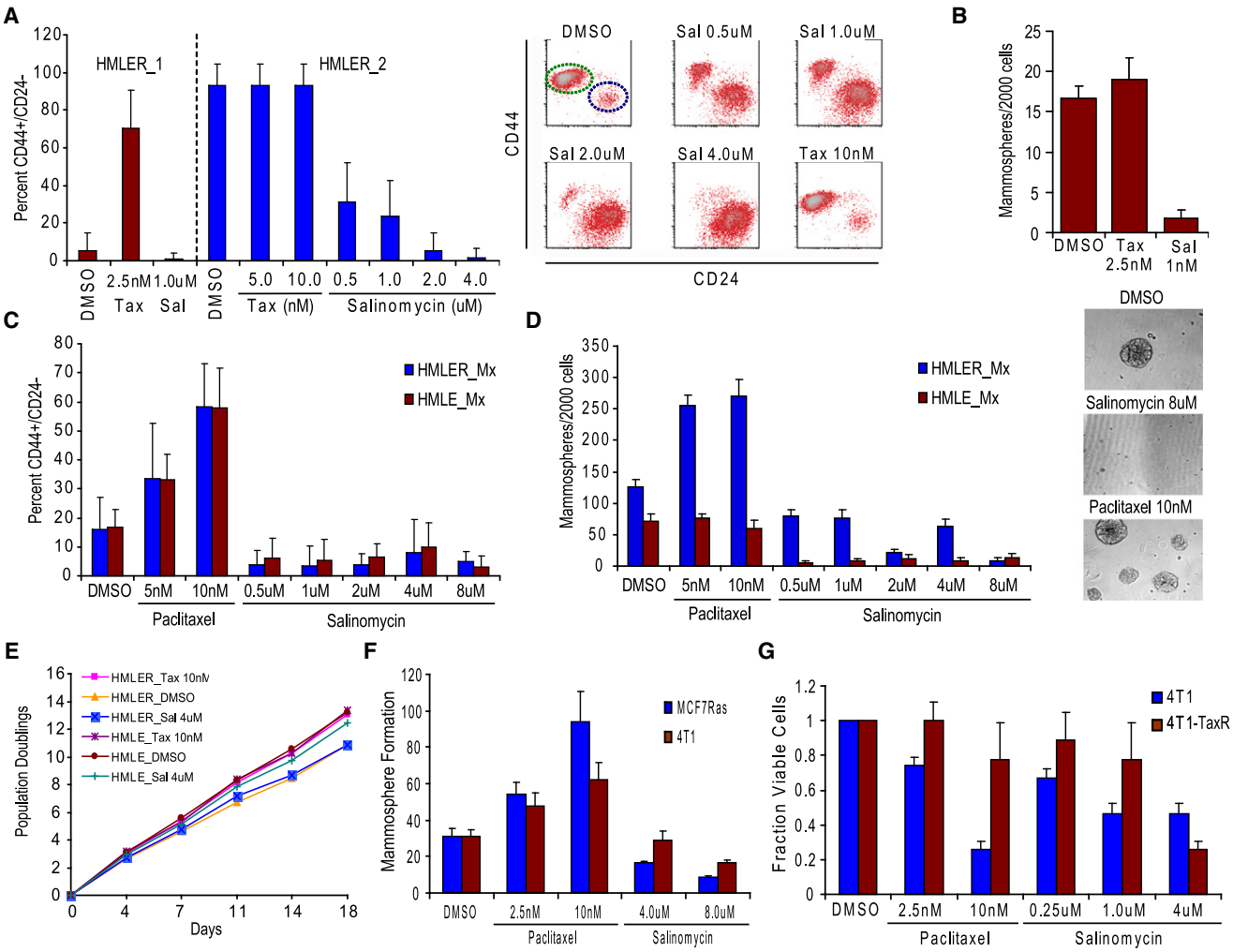

Figure 4. Effect of Salinomycin and Paclitaxel Treatment on Breast CSC Numbers

(A) HMLER cells were treated with DMSO, paclitaxel, or salinomycin at the specified doses for 4 days, and then allowed to recover in the absence of treatment for 4 days. The percent of $CD44^{high}/CD24^{low}$ cells after compound treatment in independent experiments with two different HMLER cell populations (HMLER_1, HMLER_2) is shown. Bars denote the standard error (n = 3). The CD44/CD24 FACS profiles are shown for a subset of HMLER_2 compound treatments with the green ellipse denoting the CSC-enriched fraction and the blue ellipse the CSC-depleted fraction.

(B) Quantification of tumorsphere-formation with HMLER cells treated as in (A). Bars denote the standard error for n = 5.

(C) Heterogeneous populations (control/EMT mixtures) of HMLE and HMLER cells (HMLE_Mx, HMLER_Mx, respectively) were compound treated for 4 days, cultured in the absence of compound for 4 days, and the percent of $CD44^{high}/CD24^{low}$ cells was quantified by FACS. Bars denote the standard error (n = 3).

(D) Quantification of mammosphere-formation in HMLE_Mx and HMLER_Mx populations compound-treated as in (A). Bars denote the standard error (n = 10). Phase-contrast images of mammospheres are shown.

(E) In vitro growth curves of HMLER cells compound-treated as in (A) are shown.

(F) Compound-pretreated MCF7Ras (4000 cells/well) and 4T1 cells (1000 cells/well) were seeded in the absence of compound and tumorsphere formation assessed at 10 days. Bars denote the standard error (n = 3).

(G) The fraction of viable cells after compound treatment was assessed with trypan-blue exclusion for both the parental 4T1 line and a paclitaxel-resistant 4T1 line (4T1-TaxR). Bars denote the standard error for proportions (n = 4).

In contrast, paclitaxel treatment did not affect the number of HMLE_Mx mammospheres relative to vehicle-treated controls (Figure 4D). Proliferation in monolayer cultures was not inhibited by salinomycin treatment relative to either vehicle or paclitaxel treatment (Figure 4E), indicating that salinomycin's inhibition of CSC viability was not a consequence of a general inhibition of cell proliferation.

We next examined the effects of salinomycin, paclitaxel, and DMSO treatment on two additional breast cancer cell lines—a mouse mammary tumor line (4T1) and a human breast cancer line (MCF7Ras). Salinomycin treatment led to an ~3-fold reduction in CSC numbers as gauged by tumorsphere-forming potential for MCF7Ras cells and an ~2-fold reduction for 4T1 cells relative to control DMSO treatment (Figure 4F). In contrast,

A

	Cells Injected				
	10^2	10^3	10^4	10^5	10^6
4T1-DMSO	2/8	2/8	8/8	7/8	
4T1-TAX	3/8	6/8	7/8	8/8	
4T1-SAL	0/8	0/8	5/8	8/8	
HMLER-DMSO				9/9	4/9
HMLER-TAX				9/9	11/12
HMLER-SAL				1/9	0/9

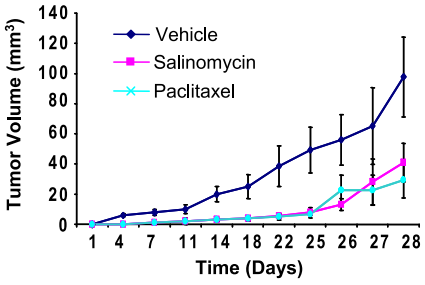

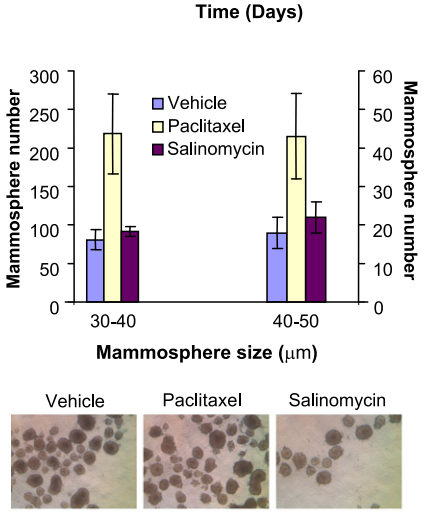

E

4T1 lung metastasis assay

Vehicle	Paclitaxel	Salinomycin
1.38 ± 0.4	3.25 ± 0.21	0.36 ± 0.04

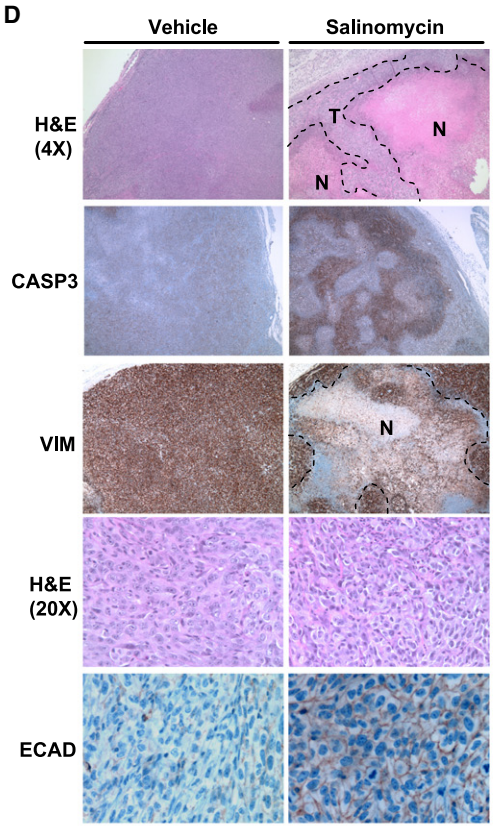

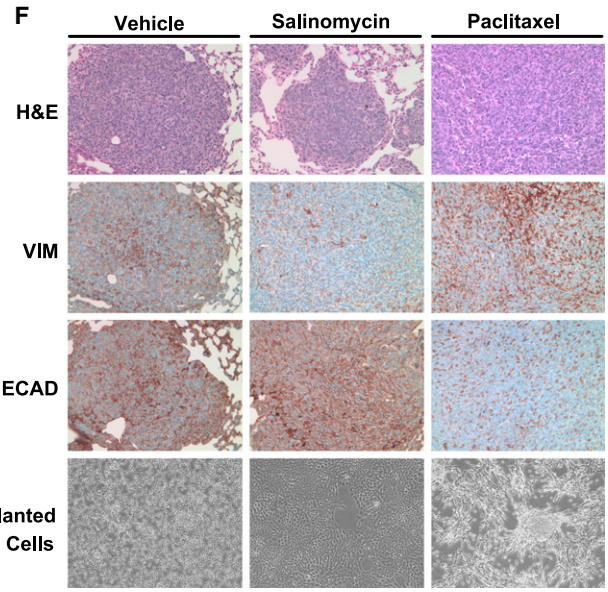

Figure 5. Effects of Salinomycin and Paclitaxel Treatment on Tumor Seeding, Growth and Metastasis In Vivo

(A) Tumor-seeding ability of HMLER and 4T1 breast cancer cells treated with salinomycin, paclitaxel, or DMSO.

(B) SUM159 tumor-growth curves of compound-treated mice. Error bars denote the standard error (n = 10).

(C) Quantification of tumorsphere-forming potential (diameter between 20 and 50 μm was evaluated) of cancer cells isolated from dissociated SUM159 tumors from compound-treated mice. Error bars denote the standard error (n = 5). Images of tumorsphere cultures are shown.

(D) Histological analysis of tumors from salinomycin- or vehicle-treated mice. Shown are H&E, caspase-3, human-specific vimentin, and E-cadherin staining.

paclitaxel treatment caused an ~3-fold increase in tumorsphere-forming potential of the MCF7Ras cells and an ~2-fold increase for 4T1 cells relative to DMSO vehicle treatment (Figure 4F). Notably, for both 4T1 and MCF7Ras cells, salinomycin treatment selected for cells with morphologic features associated with increased epithelial differentiation relative to DMSO-treated controls (Figure S4; data not shown). In contrast, paclitaxel treatment selected for cells exhibiting a mesenchymal and migratory phenotype (Figure S4).

We observed that 4T1 cells treated with paclitaxel for 4 days and then allowed to recover in the absence of drug for 4 days (4T1-TaxR cells) were resistant to further paclitaxel treatment in comparison to parental 4T1 cells that had not been previously treated with paclitaxel (Figure 4G). In contrast, the 4T1-TaxR cells, while resistant to paclitaxel, displayed a 2-fold increase in sensitivity to treatment with salinomycin in comparison to parental 4T1 cells (Figure 4G). These observations demonstrate that treatment with paclitaxel selects for mesenchymal cancer cells that display increased resistance to paclitaxel while remaining sensitive to salinomycin treatment.

Effects of Salinomycin and Paclitaxel on Tumor Seeding, Growth, and Metastasis

We also assessed the functional presence of CSCs by assaying for in vivo tumor-seeding ability after chemical compound treatment in vitro. For these experiments, HMLER and 4T1 cancer cells were treated with compounds in vitro for 7 days, allowed to recover and expand in culture for at least 14 days in the absence of treatment, and then injected in serial limiting dilutions into mice. We observed that salinomycin pretreatment resulted in a >100-fold decrease in tumor-seeding ability relative to paclitaxel pre-treatment for both the HMLER and 4T1 cancer lines (Figure 5A). These findings indicated that CSCs within breast cancer cell populations are resistant to paclitaxel but sensitive to treatment with salinomycin.

We next treated mice that had been injected orthotopically with SUM159 human breast cancer cells with paclitaxel (5 mg/kg), salinomycin (5 mg/kg), or vehicle, administered daily. While palpable tumors developed in vehicle-treated mice within ~1.5 weeks, paclitaxel and salinomycin treatment both delayed palpable tumor formation by ~2 weeks. Subsequent tumor size in salinomycin-treated animals was reduced relative to tumors in vehicle-treated animals (Figure 5B). While tumor size reduction relative to vehicle-treated controls was comparable for salinomycin- and paclitaxel-treated mice, the latter cohort exhibited a reduced tumor size at later time points (Figure 5B). Four weeks after cancer cell injection, tumors were analyzed for the presence of surviving CSCs with in vitro tumorsphere formation assays. Tumors from the paclitaxel-treated cohort had a 2-fold increase in tumorsphere-forming cells relative to either salinomycin- or vehicle-treated cohorts (Figure 5C).

Tumors from salinomycin-treated mice had increased necrosis and apoptosis compared to comparably sized tumors from vehicle-treated mice (Figure 5D). Viable cancer cells in tumors from salinomycin-treated mice were mostly restricted to the periphery of the tumor mass (Figure 5D). E-cadherin protein, which is not normally expressed in the SUM159 line, was focally expressed specifically in tumors from salinomycin-treated mice and not in tumors from control vehicle-treated mice (Figure 5D). Cells that expressed E-cadherin protein displayed a more differentiated epithelial morphology, suggesting that salinomycin treatment had either induced SUM159 cancer cells to differentiate in vivo or selected for the expansion in vivo of SUM159 cancer cell subpopulations displaying increased epithelial differentiation.

CSCs have been proposed to be responsible for colonization at secondary organ sites upon metastatic dissemination (Li et al., 2007b; Croker and Allan, 2008). We therefore examined whether the reduction in CSC numbers after salinomycin treatment was also accompanied by a reduction in metastatic nodule-forming ability. To specifically assay for the final step of metastasis, we seeded 4T1 cancer cells into the lungs of syngeneic animals via tail-vein injection. 4T1 cells pretreated in vitro with salinomycin displayed a 4-fold reduction in metastasis burden after 3 weeks growth in vivo compared to vehicle-pretreated cells (Figure 5E). In contrast, 4T1 populations pretreated with paclitaxel exhibited a 2-fold increase in metastasis formation relative to the vehicle-pretreated control cohort (Figure 5E).

We next stained lungs from 4T1 metastasis-bearing animals for markers of epithelial differentiation (E-cadherin) and EMT (vimentin). Lung nodules formed by paclitaxel-treated 4T1 cells displayed increased vimentin staining and decreased E-cadherin staining relative to nodules formed by DMSO-treated 4T1 cells (Figure 5F). In contrast, salinomycin-treated 4T1 cells formed lung nodules with increased E-cadherin and reduced vimentin expression relative to nodules formed by DMSO-treated 4T1 cells (Figure 5F). Furthermore, 4T1 cells explanted and cultured from lung nodules displayed differences in morphology; paclitaxel-treated 4T1 cells showed a mesenchymal morphology, whereas salinomycin-treated 4T1 cells showed a morphology associated with epithelial differentiation (Figure 5F). Together with our previous observations (Figure S4), these results indicated that paclitaxel and salinomycin treatment exert opposing effects on the differentiation state of breast cancer cells, with the former inducing an increase in mesenchymal transdifferentiation and the latter inducing an increase in epithelial differentiation relative to treatment with DMSO vehicle. Moreover, these alterations in differentiation state were metastable, remaining throughout the 3 week period of growth in vivo.

Reduced Expression of CSC-Associated Genes after Salinomycin Treatment

To determine whether our observations with cultured human breast cancer cells were representative of breast CSCs naturally present in mammary carcinomas, we performed comparative global gene expression analyses on three populations of HMLER

(E) Tail-vein injection of 4T1 cancer cells, pre-treated with paclitaxel, salinomycin, or DMSO. Lung images shown were captured at 1.5× magnification. Lung tumor surface area shown below the images are (mean ± SE)/10^6 for n = 5.

(F) H&E, vimentin, and E-cadherin staining of lung nodules from compound-treated 4T1 breast cancer cells. Also shown are images of cultured 4T1 cells explanted from lung nodules.

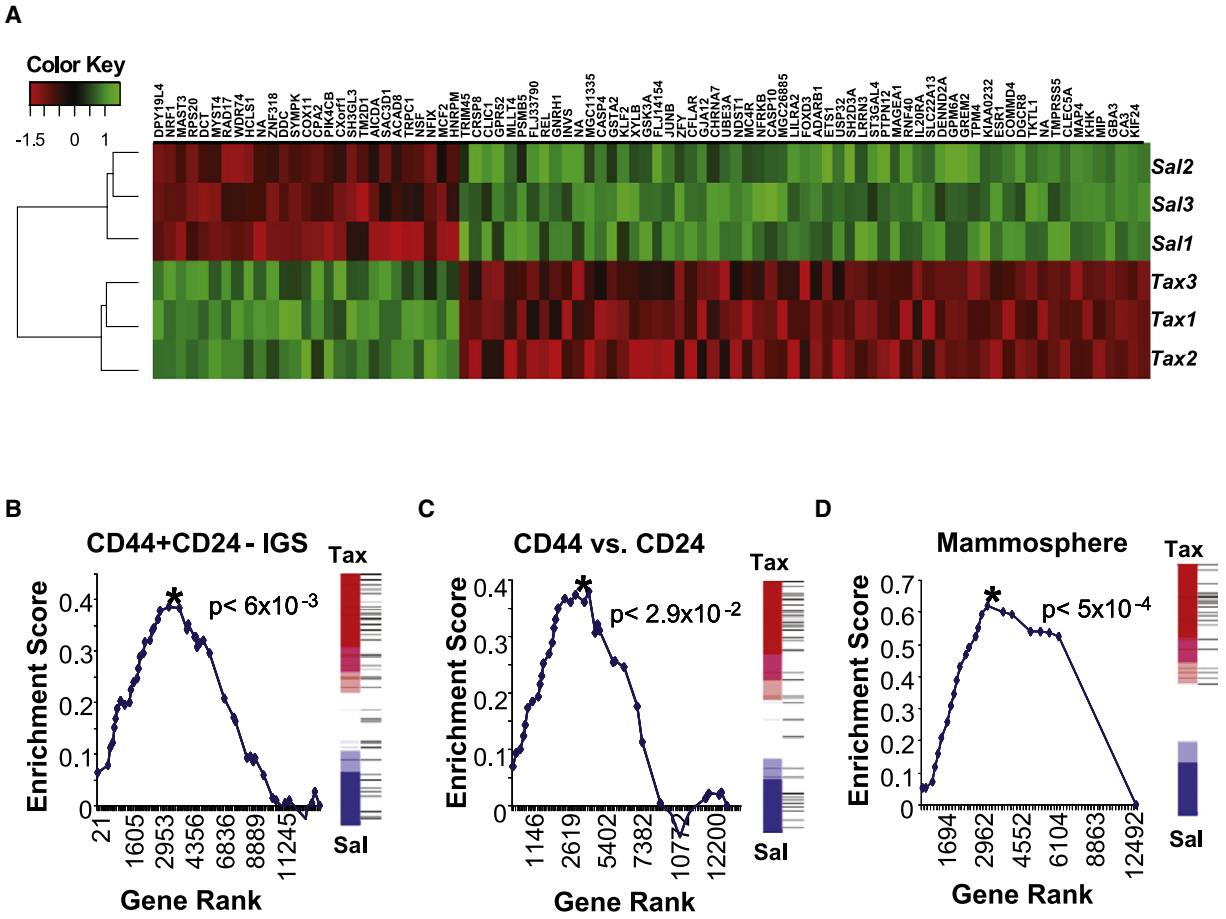

Figure 6. Salinomycin and Paclitaxel Treatment Affect Expression of CSC Genes Associated with Poor Patient Prognosis

HMLER cells were treated in triplicate with either salinomycin or paclitaxel and then subjected to microarray gene expression analysis.

(A) Genes showing differential expression ($|t$ statistic$| > 5$) between salinomycin (Sal) and paclitaxel (Tax) treatment conditions were plotted on the Heatmap using the Euclidean distance measure.

(B–D) Salinomycin treatment reduces the expression of clinically relevant breast CSC and progenitor genes. Gene set enrichment analysis was used to determine whether the previously reported $CD44^{+}CD24^{-}$ IGS (Liu et al., 2007) (B), $CD44^{+}CD24^{-}$ (Shipitsin et al., 2007) (C), or Mammosphere (Dontu et al., 2003) (D) gene sets were repressed in response to salinomycin in comparison with paclitaxel treatment. Graphed are the Kolmogorov-Smirnov enrichment scores versus Gene ranks based on differential expression. p values reflecting statistical significance for each analysis are shown. The rank of each gene in the gene set relative to the differential expression between salinomycin and paclitaxel treatment are shown as horizontal lines in the vertical bars next to each graph.

breast cancer cells treated in parallel with either salinomycin or paclitaxel (Figure 6A). We then applied gene set enrichment analysis (GSEA) (Mootha et al., 2003; Subramanian et al., 2005) to test whether genes that had been previously associated with either breast CSCs or normal mammary epithelial progenitor cells were related to those downregulated upon treatment of HMLER breast cancer cells with salinomycin relative to paclitaxel treatment.

The first gene set tested, termed the invasiveness gene signature, was generated by comparison of the expression profiles of $CD44^{high}CD24^{low}$ tumorigenic breast cancer cells with expression profiles from normal mammary epithelium (Liu et al., 2007). A previous report has suggested that this signature is correlated inversely with both metastasis-free survival and overall survival for four different types of tumors (Liu et al., 2007). The 97 genes that were upregulated in this signature constituted the $CD44^{+}CD24^{-}$ IGS gene set. GSEA revealed a significant reduction in the expression of genes in this set upon treatment with salinomycin compared with paclitaxel treatment ($p < 6 \times 10^{-3}$, $CD44^{+}CD24^{-}$ IGS gene set, Figure 6B). The second gene set, termed the CD44vs.CD24 gene set, was generated by comparing SAGE expression data from either $CD44^{high}$ or $CD24^{high}$ cells purified directly from human breast cancers (Shipitsin et al., 2007). This set consists of 41 genes upregulated in $CD44^{high}$ cells that also exhibited prognostic value for breast cancer patient clinical outcomes. GSEA indicated a significant reduction in the expression of the genes in this set upon treatment of cultured breast cancer cells with salinomycin compared with paclitaxel treatment ($p < 2.9 \times 10^{-2}$, CD44vs.CD24, Figure 6C).

The third gene set—the Mammosphere gene set (31 genes)—was obtained by comparison of the expression profiles of normal

mammary epithelial cells obtained from human patients cultured under conditions that favor mammary epithelial stem cell expansion with the expression profiles of cells cultured under conditions favoring their differentiation (Dontu et al., 2003). GSEA indicated that expression of the mammosphere-specific genes was preferentially lost upon treatment with salinomycin compared with paclitaxel treatment ($p < 5 \times 10^{-4}$, Mammosphere, Figure 6D).

The depletion of these gene sets in salinomycin-treated cells suggests an overlap between the mammary epithelial cell states associated with normal and neoplastic $CD44^{high}CD24^{low}$ cells, seeding of mammospheres, and passage through an EMT. To identify genes concordantly regulated in all of these three cell states, we compared genes exhibiting strong differential expression in (1) paclitaxel- versus salinomycin-treated HMLER cells, (2) primary human mammary epithelial cells grown in suspension sphere versus adherent culture conditions (Dontu et al., 2003), and (3) CD44+ versus CD24+ normal and neoplastic primary human mammary epithelial cells (Shipitsin et al., 2007).

We found 25 genes that showed more than 3-fold upregulation across all three of the comparisons and 14 genes that showed a greater than 3-fold downregulation across all three comparisons (Table 1). Notably, almost all of the coordinately regulated genes encoded proteins that were either membrane-associated or secreted factors, the latter of which included multiple components of the extracellular matrix. This indicates that these genes and their products are associated with specific phenotypes of the normal and neoplastic stem cell states.

DISCUSSION

Given the variety of therapies to which they are resistant, it is possible that CSCs would exhibit a generalized resistance to apoptosis, suggesting that it might not be possible in practice to find therapies that specifically target CSCs. Here, we demonstrate that this is not the case and that it is in fact possible to use unbiased screening strategies to systematically identify chemical compounds that specifically target breast CSCs. The approach described here can be extended to other epithelial cancer types and implemented using any reagent collection compatible with high-throughput screening, including RNA interference (RNAi), antibody, or complementary DNA (cDNA)-overexpression libraries.

As shown here, salinomycin preferentially targets the viability of CSCs within breast cancer cell populations. Moreover, salinomycin but not paclitaxel treatment results in the loss of expression of CSC-associated genes correlated with poor-prognosis tumors. This finding indicates that breast CSCs in culture have a molecular phenotype that reflects the in vivo biology of CSCs, since the poor-prognosis CSC-associated gene sets examined here were compiled from two independent studies using tissues isolated directly from patients. Moreover, the subset of genes coordinately expressed in CSCs and downregulated in salinomycin-treated cells (Table 1) may serve as useful biomarkers for identifying breast tumors that would be responsive to anti-CSC therapies.

The screen reported here was carried out with genetically well-defined immortalized mammary epithelial cells that were not tumorigenic. This experimental design was adopted to minimize the likelihood of finding compounds that depend on undefined genetic alterations in order to selectively kill cells that have undergone an EMT. The observation that compounds identified by screening with nontumorigenic cells also target CSCs provides further evidence linking the CSC state with EMT (Mani et al., 2008). Moreover, this observation suggests a new avenue for the development of antitumor therapies. To date, rational cancer therapies have been designed to target specific genetic alterations present within tumors. The findings here indicate that a second approach may also prove useful—namely, searching for agents that target specific states of cancer cell differentiation. Accordingly, future therapies could offer greater possibilities for individualized treatment by considering both the genetic alterations and differentiation states present within the cancer cells of a tumor at the time of diagnosis.

The mechanism(s) by which salinomycin, a potassium ionophore, induces breast CSC-specific toxicity remains unclear. Nigericin, another potassium ionophore bearing structural similarity to salinomycin, also exhibited selective toxicity for $HMLE^{shEcad}$ cells both in our primary screen and in follow-up validation. Further studies will be required to characterize the connection between potassium membrane potential and CSC biology.

An important future direction would be extending the findings reported here to primary tumor cells directly explanted from patients. However, such studies will have to surmount two significant technical challenges: (1) only ~20% of patient-derived breast cancers can currently be successfully engrafted directly into immunocompromised murine hosts and (2) the genetic and histopathologic variability among patient tumors at the time of surgical resection would confound any comparisons of the effects of drug treatment across different xenograft-bearing animals in vivo. Thus, such an experimental design would require a large number of primary tumor samples derived from patients diagnosed with the same subtype of breast cancer and would ideally stratify for genetic background.

The importance of targeting CSCs derives from the multiple observations showing that CSCs, in addition to having increased tumor-seeding potential, are resistant to a variety of chemotherapy drugs and radiation treatment. As is shown here and elsewhere (Fillmore and Kuperwasser, 2008), treatment with paclitaxel actually imposes a strong selection for CSC survival and expansion. This suggests that in cases where chemotherapy or radiation treatment fail to completely eradicate the disease, the residual cancer cells will be highly enriched for cells that persist in a CSC/mesenchymal state. This notion is supported by recent clinical observations showing that after conventional chemotherapy, breast tumors have an increased proportion of cells with a $CD44^{hi}/CD24^{lo}$ marker profile and increased tumorsphere-forming ability (Li et al., 2008). Collectively, these considerations indicate that to be effective in the long-term, cancer therapies should include agents that target CSCs to prevent the regrowth of neoplastic cell populations.

It is conceivable that non-CSCs within tumors can give rise to CSCs at a low but significant rate. It is also possible that the elimination of the CSCs within a tumor may not result in its complete regression, since non-CSCs, while less aggressive,

Table 1. Genes Differentially Expressed in Both Compound-Treated—Paclitaxel versus Salinomycin—Cancer Cells and in Normal and Neoplastic Breast Epithelial Populations Enriched for Stem-like Cells

Affymetrix ProbeID	Paclitaxel vs. Salinomycin	Sphere vs. Adherent	CD44+ vs. CD24+	Gene Symbol	Gene Description
Upregulated in Breast CSCs					
202403_s_at	21.53	4.51	22.1	COL1A2	collagen, type I, alpha 2
209392_at	16.99	4.88	18.65	ENPP2	ectonucleotide pyrophosphatase
202465_at	12.8	22.67	5.22	PCOLCE	procollagen endopeptidase enhancer
207173_x_at	11.21	14.93	20.15	CDH11	cadherin 11, type 2, OB-cadherin
209156_s_at	9.2	21.87	22.68	COL6A2	collagen, type VI, alpha 2
202283_at	9	12.06	24.62	SERPINF1	serpin peptidase inhibitor, clade F
212667_at	8.59	4.24	24.27	SPARC	secreted protein, acidic, cysteine-rich
202766_s_at	8.19	5.13	21.64	FBN1	fibrillin 1
218162_at	7.39	>10	15.33	OLFML3	olfactomedin-like 3
202310_s_at	6.4	17.31	19.37	COL1A1	collagen, type I, alpha 1
212158_at	6.27	4.99	5.97	SDC2	syndecan 2
213869_x_at	5.87	>10	52.34	THY1	Thy-1 cell surface antigen
212154_at	5.82	5.36	5.97	SDC2	syndecan 2
201508_at	4.76	8.5	8.78	IGFBP4	insulin-like growth factor BP4
212091_s_at	4.69	>10	15.86	COL6A1	collagen, type VI, alpha 1
203186_s_at	4.52	6.73	6.31	S100A4	S100 calcium binding protein A4
211981_at	4.28	>10	31.52	COL4A1	collagen, type IV, alpha 1
210809_s_at	4.23	5.55	36.56	POSTN	periostin
212298_at	4.1	5.11	8.95	NRP1	neuropilin 1
211966_at	4.01	>10	31.52	COL4A2	collagen, type IV, alpha 2
211709_s_at	3.82	3.53	18.65	CLEC11A	C-type lectin domain family 11
201525_at	3.71	>10	11.96	APOD	apolipoprotein D
203729_at	3.62	6.12	5.21	EMP3	epithelial membrane protein 3
210201_x_at	3.38	3.07	17.14	BIN1	bridging integrator 1
209081_s_at	3.19	31.08	10.11	COL18A1	collagen, type XVIII, alpha 1
Downregulated in Breast CSCs					
209529_at	−3.48	<-10	−6.62	PPAP2C	phosphatidic acid phosphatase 2C
219976_at	−3.64	<-10	−4.96	HOOK1	hook homolog 1 (*Drosophila*)
202023_at	−5.46	<-10	−5.54	EFNA1	ephrin-A1
205286_at	−5.76	−3.62	−8.27	TFAP2C	transcription factor AP-2 gamma
201688_s_at	−5.9	<−10	−4.99	TPD52	tumor protein D52
210715_s_at	−7.47	−3.28	−9.34	SPINT2	serine peptidase inhibitor, Kunitz
219850_s_at	−8.32	−4.97	−14.41	EHF	ets homologous factor
208083_s_at	−8.86	<−10	−15.89	ITGB6	integrin, beta 6
207291_at	−9.56	<−10	−14.41	PRRG4	proline rich G-carboxyglutamic acid4
203780_at	−9.86	−7.23	−17.74	EVA1	epithelial V-like antigen 1
204351_at	−19.86	−4.01	−12.57	S100P	S100 calcium binding protein P
201839_s_at	−32.09	−4.59	−9.98	TACSTD1	tumor-assoc. ca signal transducer 1
202489_s_at	−36.28	−3.28	−10.64	FXYD3	FXYD domain ion transport reg 3
209772_s_at	−49.1	−3.69	−28.73	CD24	CD24 molecule

Genes with >3-fold differential expression across all three comparisons are shown, together with the extent of differential expression in each data set. The data are from (1) paclitaxel- versus salinomycin-treated HMLER cells, (2) primary human mammary epithelial cells grown either in suspension colonies or in adherent conditions (Dontu et al., 2003), and (3) normal and neoplastic human mammary epithelial populations enriched for either CD44+ or CD24+ cells (Shipitsin et al., 2007). Genes reported in Dontu et al. (2003) as being expressed in only one of the two conditions compared are shown as having a greater than 10-fold change in expression.

may nonetheless be capable of maintaining an already-established tumor for an extended period of time. Either of these possibilities would compromise the therapeutic utility of agents that exclusively target CSCs. One strategy to address this concern would be to look for agents that target both the CSCs and non-CSCs within tumors. Alternatively, it may be preferable to develop combination therapies that apply agents with specific toxicity for CSCs together with agents that specifically target non-CSC populations within tumors.

Due to practical considerations related to compound availability, the current study was focused largely on the anti-CSC properties of a single agent, salinomycin. However, our experiments indicate that ~30% of the primary screen hits exhibit EMT-specific toxicity upon retesting. Therefore, it is likely that expanding the breadth and scope of the current screen to larger library collections will result in the discovery of additional agents of therapeutic interest.

EXPERIMENTAL PROCEDURES

Cell Culture

HMLE and HMLER cells expressing either control shRNA (shCntrl) or shRNA targeting E-cadherin (shEcad) were generated and maintained in a 1:1 mixture of DMEM + 10% FBS, insulin, hydrocortisone, and MEGM. GFP-expressing HMLE and HMLE-shEcad cell strains were generated by infection with retrovirus encoding the pWZL-GFP plasmid. SUM159 cells (Asterand) were cultured in F12 + 5% FBS, insulin, and hydrocortisone. 4T1 cells (ATCC) were maintained in RPMI + 10% FBS.

Mammosphere formation assays were performed as described (Dontu et al., 2003), but with 0.5% methylcellulose (Stem Cell Technologies). One thousand cells were plated per well in low-adherence 96-well plates and cultured for 7–10 days prior to being counted and photographed.

Antibodies

Antibodies used for immunoblotting were as follows: E-cadherin, N-cadherin (BD Transduction), Vimentin V9 (NeoMarkers), Actin (Abcam), H-Ras (Santa Cruz), and Cytokeratin 8 (Troma-1, Developmental Studies Hybridoma Bank, University of Iowa). Western blotting was performed as previously described (Onder et al., 2008). Antibodies used for immunohistochemistry were as follows: pan-cytokeratin (clones AE1/AE3&PCK26, Ventana Medical Systems), Vimentin (3B4, Ventana and V9, Vector Labs), caspase-3 (Asp175, Cell Signaling), and E-cadherin (ECH-6, Ventana and Vector Labs). Immunohistochemistry procedures were performed as previously described (Gupta et al., 2005).

Fluorescence-Activated Cell Sorting

APC-conjugated anti-CD44 (clone G44-26) antibody, PE-conjugated anti-CD24 antibody (clone ML5), and propidium iodide (5 μg/ml) were obtained from BD Biosciences and used for fluorescence-activated cell sorting (FACS) analysis in accordance with the manufacturer's protocols.

Characterization of Resistance to Cytotoxic Agents

All compounds were purchased from Sigma and dissolved in DMSO. Cells (5000/well) were plated in 100 μl per well in 96-well plates. One day (24 hr) after seeding, compounds were added in five replicates per concentration for each cell line. Cell viability was measured after 72 hr with the CellTiter96 AQueous Non-radioactive Assay (Promega).

For cell mixture experiments, unlabeled and GFP-labeled cells were mixed and seeded into 6-well plates. Wells were compound treated in triplicate for 48 hr prior to FACS.

Chemical Screen and Analysis

Chemical screening was conducted at the Chemical Biology Platform of the Broad Institute. Cells were seeded in 40 μl of medium containing 1000 cells per well into white 384-well opaque-bottom plates (Nunc, Rochester, NY) using an automated plate filler (Bio-Tek μFiller; Winsooki, VT). At 24 hr, 100 nL of compound solutions were pin transferred from stock 384-well plates into the 384-well assay plates containing cells, resulting in ~10 μM final concentration for most compounds.

The HMLE^{shCntrl} and HMLE^{shEcad} lines were each screened in two replicates. Two kinds of negative control wells were employed for normalization: multiple DMSO-only control wells (>10% of wells/plate) were present on each compound assay plate screened, and all wells in at least one assay plate for each cell line were also treated with DMSO alone. CellTiter-Glo Reagent (Promega) was added 3 days after compound addition (20 μl/well). Luminescence signal was measured with an automated plate reader (Perkin-Elmer Envision 1).

The raw intensity data for each well were background-corrected by subtraction of the median intensities across all control wells on the same plate. The background-corrected data were used to compute a per-well Z score by subtraction of the per-plate mean and division by twice the per-replicate standard deviation. Composite Z scores for each compound/cell line combination were computed by projection of the vector of normalized replicate Z scores (ZscoreA, ZscoreB) onto the imaginary vector corresponding to perfect reproducibility.

Internal compound plate numbers for screened plates were 2158–2167, 2099–2105, 2290–2297, 2403–2407, and Biokin1-2. Primary screening data have been deposited into Chembank (Screen ID: 1108), a publicly accessible database (http://chembank.broad.harvard.edu/).

Follow-up Validation of Compounds from Primary Screen

All compounds for follow-up were purchased from Sigma and dissolved in DMSO, with the exception of Nigericin, which was dissolved in 100% ethanol. Activity of the compounds were quantified by generation of dose-response curves for HMLE-shCntrl, HMLE-shEcad, and HMLE-Twist under the same cell density and culture conditions described for the initial screen.

Animal Experiments

NOD/SCID and Balb/c mice were purchased from Jackson Labs. All mouse procedures were approved by the Animal Care and Use Committees of the Massachusetts Institute of Technology and Tufts University School of Medicine and performed in accordance with institutional policies.

For xenograft tumor-seeding studies, the indicated numbers of HMLER-shCntrl, HMLER-shEcad, or drug-treated (DMSO vehicle control; 10 nM paclitaxel; 1 μM salinomycin) HMLER cells were suspended in 100 μl Matrigel diluted 1:2 in DMEM and injected subcutaneously into NOD-SCID mice. For drug pretreatment experiments, parental HMLER cells were treated for 1 week and allowed to recover in the absence of drug for 2 weeks prior to injection in vivo. Tumor incidence was monitored for 60 days after injection. For syngeneic tumor seeding studies, 4T1 cells were pretreated for 4 days with paclitaxel (10 nM), salinomycin (4 μM), or DMSO in vitro. Cells were injected in 30 μl 1:1 Matrigel:DMEM solution into the thoracic and inguinal mammary glands. For tail-vein injection, 1×10^5 4T1 cells were resuspended in 100 μl saline. Tumor formation was assayed by palpation. Tumor and tissues were fixed in 10% buffered formalin. Lung tumor burden was quantified using Spot Software v4.1.3 on captured images to calculate the mean tumor surface area.

For in vivo compound treatment studies, 1×10^6 SUM159 cells were resuspended in F12 medium and injected into the fourth inguinal mammary glands of NOD/SCID mice. Compound treatment was initiated 24 hr after injection. Animals were administered either ethanol (vehicle), salinomycin (5 mg/kg), or paclitaxel (5 mg/kg) daily by intraperitoneal injection for 5 weeks.

Tumor Cell Isolation and Tumorsphere Assays

SUM159 tumor tissues were minced and digested for 3 hr with agitation at 37°C with collagenase and hyaluronidase. Single-cell suspensions were plated (30,000 cells/well) in 6-well ultra-low attachment plates (Corning) in F12 + 5% FBS, insulin, and hydrocortisone. Tumorspheres were cultured for 8 days. Tumorspheres collected from nonadherent cultures were quantified with a Multisizer 3 Coulter Counter (sizing range of 14–336 μm).

4T1 lung nodules were isolated at necropsy under a dissection microscope. Lung nodules were minced and dissociated 4T1 cells plated in DMEM + 10% FBS for 7 days.

Microarray Data Collection and Gene Expression Analyses

HMLER breast cancer cells were drug-treated for 1 week (10 nM paclitaxel; 1 μM salinomycin) and cultured in the absence of drug for 3 weeks prior to RNA isolation. Total RNA was isolated with the RNeasy Mini kit (QIAGEN). Synthesis of cRNA from total RNA and hybridization/scanning of microarrays were performed with Affymetrix GeneChip products (HGU133A) as described in the GeneChip manual. Normalization of the raw gene expression data, quality control checks, and subsequent analyses were done with the open-source R-project statistical software (R Development Core Team, 2007) (http://www.r-project.org/) together with Bioconductor packages. Raw data files (.CEL) were converted into probe set values by RMA normalization.

After RMA normalization, the t statistic was used to generate a ranked list of genes that are differentially expressed between salinomycin-treated and paclitaxel-treated HMLER cells. GSEA was performed with this preranked list as described previously (Mootha et al., 2003; Subramanian et al., 2005). The gene sets used for the analysis were compiled from published sources (Dontu et al., 2003; Liu et al., 2007; Shipitsin et al., 2007) and are provided in Table S1.

ACCESSION NUMBERS

The gene expression microarray data reported in this paper have been deposited in the Gene Expression Omnibus (GEO) repository with accession number GSE17215.

SUPPLEMENTAL DATA

Supplemental Data include five figures and one table and can be found with this article online at http://www.cell.com/supplemental/S0092-8674(09)00781-8.

ACKNOWLEDGMENTS

We thank the National Cancer Institute and the Initiative for Chemical Genetics, who provided support for this publication, and the Chemical Biology Platform of the Broad Institute of Harvard and the Massachusetts Institute of Technology (MIT) for their assistance in this work. We also wish to thank David Root and the RNAi Platform of the Broad Institute as well as the Breast Cancer Research Foundation for their support. We are grateful to Stephanie Norton, Nicola Tolliday, and Paul Clemons for assistance with chemical screening experiments and analysis. We thank Ina Klebba for assistance with animal experiments, Annette Shepard-Barry in the Histology-Special Procedures Lab at Tufts Medical Center for histological and immunohistochemical staining, Tugba Bagci Onder for help with initial drug resistance characterization, and Supriya Gupta in the Genetic Analysis Platform at the Broad Institute for assistance with gene expression microarray data collection. We thank Li Li in the Department of Chemistry Instrumentation Facility at MIT for fourier-transform mass spectrometry analysis and Dr. Sagi Shapira for helpful criticism of the manuscript.

Received: October 21, 2008
Revised: February 18, 2009
Accepted: June 12, 2009
Published online: August 13, 2009

REFERENCES

Al-Hajj, M., Wicha, M.S., Benito-Hernandez, A., Morrison, S.J., and Clarke, M.F. (2003). Prospective identification of tumorigenic breast cancer cells. Proc. Natl. Acad. Sci. USA *100*, 3983–3988.

Bao, S., Wu, Q., McLendon, R.E., Hao, Y., Shi, Q., Hjelmeland, A.B., Dewhirst, M.W., Bigner, D.D., and Rich, J.N. (2006). Glioma stem cells promote radioresistance by preferential activation of the DNA damage response. Nature *444*, 756–760.

Croker, A.K., and Allan, A.L. (2008). Cancer stem cells: implications for the progression and treatment of metastatic disease. J. Cell. Mol. Med. *12*, 374–390.

Dean, M., Fojo, T., and Bates, S. (2005). Tumour stem cells and drug resistance. Nat. Rev. Cancer *5*, 275–284.

Diehn, M., and Clarke, M.F. (2006). Cancer stem cells and radiotherapy: new insights into tumor radioresistance. J. Natl. Cancer Inst. *98*, 1755–1757.

Diehn, M., Cho, R.W., Lobo, N.A., Kalisky, T., Dorie, M.J., Kulp, A.N., Qian, D., Lam, J.S., Ailles, L.E., Wong, M., et al. (2009). Association of reactive oxygen species levels and radioresistance in cancer stem cells. Nature *458*, 780–783.

Dontu, G., Abdallah, W.M., Foley, J.M., Jackson, K.W., Clarke, M.F., Kawamura, M.J., and Wicha, M.S. (2003). In vitro propagation and transcriptional profiling of human mammary stem/progenitor cells. Genes Dev. *17*, 1253–1270.

Elenbaas, B., Spirio, L., Koerner, F., Fleming, M.D., Zimonjic, D.B., Donaher, J.L., Popescu, N.C., Hahn, W.C., and Weinberg, R.A. (2001). Human breast cancer cells generated by oncogenic transformation of primary mammary epithelial cells. Genes Dev. *15*, 50–65.

Eyler, C.E., and Rich, J.N. (2008). Survival of the fittest: cancer stem cells in therapeutic resistance and angiogenesis. J. Clin. Oncol. *26*, 2839–2845.

Fillmore, C.M., and Kuperwasser, C. (2008). Human breast cancer cell lines contain stem-like cells that self-renew, give rise to phenotypically diverse progeny and survive chemotherapy. Breast Cancer Res. *10*, R25.

Gupta, P.B., Kuperwasser, C., Brunet, J.P., Ramaswamy, S., Kuo, W.L., Gray, J.W., Naber, S.P., and Weinberg, R.A. (2005). The melanocyte differentiation program predisposes to metastasis after neoplastic transformation. Nat. Genet. *37*, 1047–1054.

Lapidot, T., Sirard, C., Vormoor, J., Murdoch, B., Hoang, T., Caceres-Cortes, J., Minden, M., Paterson, B., Caligiuri, M.A., and Dick, J.E. (1994). A cell initiating human acute myeloid leukaemia after transplantation into SCID mice. Nature *367*, 645–648.

Levina, V., Marrangoni, A.M., DeMarco, R., Gorelik, E., and Lokshin, A.E. (2008). Drug-selected human lung cancer stem cells: cytokine network, tumorigenic and metastatic properties. PLoS ONE *3*, e3077.

Li, C., Heidt, D.G., Dalerba, P., Burant, C.F., Zhang, L., Adsay, V., Wicha, M., Clarke, M.F., and Simeone, D.M. (2007a). Identification of pancreatic cancer stem cells. Cancer Res. *67*, 1030–1037.

Li, F., Tiede, B., Massague, J., and Kang, Y. (2007b). Beyond tumorigenesis: cancer stem cells in metastasis. Cell Res. *17*, 3–14.

Li, X., Lewis, M.T., Huang, J., Gutierrez, C., Osborne, C.K., Wu, M.F., Hilsenbeck, S.G., Pavlick, A., Zhang, X., Chamness, G.C., et al. (2008). Intrinsic resistance of tumorigenic breast cancer cells to chemotherapy. J. Natl. Cancer Inst. *100*, 672–679.

Liu, R., Wang, X., Chen, G.Y., Dalerba, P., Gurney, A., Hoey, T., Sherlock, G., Lewicki, J., Shedden, K., and Clarke, M.F. (2007). The prognostic role of a gene signature from tumorigenic breast-cancer cells. N. Engl. J. Med. *356*, 217–226.

Mani, S.A., Guo, W., Liao, M.J., Eaton, E.N., Ayyanan, A., Zhou, A.Y., Brooks, M., Reinhard, F., Zhang, C.C., Shipitsin, M., et al. (2008). The epithelial-mesenchymal transition generates cells with properties of stem cells. Cell *133*, 704–715.

Mootha, V.K., Lindgren, C.M., Eriksson, K.F., Subramanian, A., Sihag, S., Lehar, J., Puigserver, P., Carlsson, E., Ridderstrale, M., Laurila, E., et al. (2003). PGC-1alpha-responsive genes involved in oxidative phosphorylation are coordinately downregulated in human diabetes. Nat. Genet. *34*, 267–273.

Onder, T.T., Gupta, P.B., Mani, S.A., Yang, J., Lander, E.S., and Weinberg, R.A. (2008). Loss of E-cadherin promotes metastasis via multiple downstream transcriptional pathways. Cancer Res. *68*, 3645–3654.

R Development Core Team. (2007). R: A Language and Environment for Statistical Computing. (Vienna, Austria: R Foundation for Statistical Computing).

Ricci-Vitiani, L., Lombardi, D.G., Pilozzi, E., Biffoni, M., Todaro, M., Peschle, C., and De Maria, R. (2007). Identification and expansion of human colon-cancer-initiating cells. Nature *445*, 111–115.

Shipitsin, M., Campbell, L.L., Argani, P., Weremowicz, S., Bloushtain-Qimron, N., Yao, J., Nikolskaya, T., Serebryiskaya, T., Beroukhim, R., Hu, M., et al. (2007). Molecular definition of breast tumor heterogeneity. Cancer Cell *11*, 259–273.

Singh, S.K., Clarke, I.D., Terasaki, M., Bonn, V.E., Hawkins, C., Squire, J., and Dirks, P.B. (2003). Identification of a cancer stem cell in human brain tumors. Cancer Res. *63*, 5821–5828.

Smalley, M., and Ashworth, A. (2003). Stem cells and breast cancer: a field in transit. Nat. Rev. Cancer *3*, 832–844.

Stingl, J., and Caldas, C. (2007). Molecular heterogeneity of breast carcinomas and the cancer stem cell hypothesis. Nat. Rev. Cancer *7*, 791–799.

Subramanian, A., Tamayo, P., Mootha, V.K., Mukherjee, S., Ebert, B.L., Gillette, M.A., Paulovich, A., Pomeroy, S.L., Golub, T.R., Lander, E.S., et al. (2005). Gene set enrichment analysis: a knowledge-based approach for interpreting genome-wide expression profiles. Proc. Natl. Acad. Sci. USA *102*, 15545–15550.

Thomson, S., Buck, E., Petti, F., Griffin, G., Brown, E., Ramnarine, N., Iwata, K.K., Gibson, N., and Haley, J.D. (2005). Epithelial to mesenchymal transition is a determinant of sensitivity of non-small-cell lung carcinoma cell lines and xenografts to epidermal growth factor receptor inhibition. Cancer Res. *65*, 9455–9462.

Woodward, W.A., Chen, M.S., Behbod, F., Alfaro, M.P., Buchholz, T.A., and Rosen, J.M. (2007). WNT/beta-catenin mediates radiation resistance of mouse mammary progenitor cells. Proc. Natl. Acad. Sci. USA *104*, 618–623.

Yang, A.D., Fan, F., Camp, E.R., van Buren, G., Liu, W., Somcio, R., Gray, M.J., Cheng, H., Hoff, P.M., and Ellis, L.M. (2006). Chronic oxaliplatin resistance induces epithelial-to-mesenchymal transition in colorectal cancer cell lines. Clin. Cancer Res. *12*, 4147–4153.

Yang, J., Mani, S.A., Donaher, J.L., Ramaswamy, S., Itzykson, R.A., Come, C., Savagner, P., Gitelman, I., Richardson, A., and Weinberg, R.A. (2004). Twist, a master regulator of morphogenesis, plays an essential role in tumor metastasis. Cell *117*, 927–939.

Yauch, R.L., Januario, T., Eberhard, D.A., Cavet, G., Zhu, W., Fu, L., Pham, T.Q., Soriano, R., Stinson, J., Seshagiri, S., et al. (2005). Epithelial versus mesenchymal phenotype determines in vitro sensitivity and predicts clinical activity of erlotinib in lung cancer patients. Clin. Cancer Res. *11*, 8686–8698.

Zhang, M., Behbod, F., Atkinson, R.L., Landis, M.D., Kittrell, F., Edwards, D., Medina, D., Tsimelzon, A., Hilsenbeck, S., Green, J.E., et al. (2008). Identification of tumor-initiating cells in a p53-null mouse model of breast cancer. Cancer Res. *68*, 4674–4682.